Available online at www.sciencedirect.com
SCIENCE DIRECT®
International Journal of Heat and Mass Transfer 49 (2006) 2924–2930
International Journal of HEAT and MASS TRANSFER
www.elsevier.com/locate/ijhmt

Characterization of transition to turbulence in microchannels

C. Rands, B.W. Webb *, D. Maynes

Department of Mechanical Engineering, Brigham Young University, Provo, UT 84602-4201, USA

Received 28 September 2005; received in revised form 8 February 2006
Available online 18 April 2006

Abstract

This paper reports on an experimental study characterizing the laminar-turbulent transition for water flow in circular microtubes. Microtubes with diameters in the range 16.6–32.2 μm of varying length were employed over the Reynolds number range 300–3400. The volume flowrate was measured for an imposed pressure differential using a timed displacement technique. Additionally, the viscous heating-induced mean fluid temperature rise was measured. Two independent approaches were used to identify transition from laminar to turbulent flow. Both methods showed transition to occur in the Reynolds number range 2100–2500, consistent with macroscale tube flow behavior.
© 2006 Elsevier Ltd. All rights reserved.

1. Introduction

Recent progress in development and application of microdevices has provided motivation for improved understanding of fluid transport at the microscale. Examples of typical microdevice uses include chemical detection and separation processes and high performance electronics cooling techniques. An issue that has received much attention is whether conventional macroscale flow behavior can be utilized to predict flow in microchannels. More specifically, several studies have sought to determine whether effects which may become significant at the microscale influence the transition from laminar to turbulent flow. Sharp and Adrian [1] point out that such phenomena as acoustic disturbances, vibrations, inlet agitation, and molecular motion are not clearly understood in the context of transition to turbulence. Further, the impact of microtube surface roughness is not well characterized at the microscale. It is readily acknowledged that for macroscale flows the frictional pressure drop is considerably higher in the turbulent flow regime. Thus, while the required pressure to generate laminar flow at the microscale is very high, after the onset of turbulent flow the required driving pressure becomes even greater. Consequently, there is considerable incentive to characterize the transition from laminar to turbulent flow in microchannels of physical scales 100 μm or less.

Although classical theory implies that scale has little effect on flow conditions, some prior work has concluded that transition to turbulence may occur at a critical Reynolds number (Re_{cr}) in microchannels lower than that commonly accepted for macroscale flows. While many investigations report deviations in laminar and turbulent friction factor in microchannels from conventional macroscale data, the review of prior work presented here focuses exclusively on observations of transition to turbulence at such physical scales. The most common method of experimentally identifying transition to turbulence is the observed deviation of the friction factor-Reynolds number product from the constant value observed in laminar flow. Based on both frictional pressure drop [2] and heat transfer [3] measurements in rectangular microchannels micromachined in stainless steel substrates of hydraulic diameter ranging from 133 to 367 μm, Peng et al. observed that transition occurs at Reynolds numbers in the range 300–800. The experimental data of Harms et al. in deep rectangular microchannels of width 251 μm fabricated using chemical etching of silicon substrates suggest onset of turbulence at a critical Reynolds number $Re_{cr} = 1500$ [4]. Hsieh et al. observed transition to turbulence at a Reynolds number

* Corresponding author. Tel.: +1 801 422 6543; fax: +1 801 422 0516.
E-mail address: webb@byu.edu (B.W. Webb).

0017-9310/$ - see front matter © 2006 Elsevier Ltd. All rights reserved.
doi:10.1016/j.ijheatmasstransfer.2006.02.032

Nomenclature

c_p	fluid specific heat
D	microtube diameter
D_h	hydraulic diameter
Ec	Eckert number, $\bar{u}^2/c_p(T_{m,o} - T_{m,i})$
f	Darcy friction factor
K_L	minor loss coefficient
L	microtube length
L_{fd}	hydrodynamic development length
P	pressure
R	microtube radius
Re	Reynolds number, $\rho\bar{u}D_h/\mu$
Re_{cr}	critical Reynolds number
$T_{m,i}$	mixed-mean fluid temperature at the microtube inlet
$T_{m,o}$	mixed-mean fluid temperature at the microtube outlet
t	time
$\bar{u}$	mean fluid velocity in tube
V	volume

Greek symbols

μ	liquid viscosity
ρ	liquid density

of 240 in a rectangular microchannel of hydraulic diameter 146 μm fabricated from PMMA substrates using frictional pressure drop measurements [5]. Mala and Li explored fluid flow in stainless steel and fused silica microtubes of diameter in the range 50–254 μm [6]. Transition was observed to occur at a critical Reynolds number between 300 and 900, depending on tube material. Based on local velocity measurements using micro-PIV in rectangular silicon microchannels of hydraulic diameter 50–300 μm, Zeighami et al. concluded that the onset of transition occurs in the Reynolds number range 1200–1600 [7]. This is in agreement with the work of Li et al. [8], whose micro-PIV measurements in PDMS microchannels of hydraulic diameter 325 μm suggested a critical Reynolds number of 1540. Based on pressure drop measurements in high-aspect-ratio microchannels of polycarbonate top plate and polyimide bottom plate with depth ranging from 128 to 1050 μm, Pfund et al. concluded that transition to turbulence occurred at Reynolds numbers lower than the critical Reynolds number for macroscale ducts, in the range $Re_{cr} =$ 1500–2100 [9].

Other work concludes that there are no statistically observable differences in the critical Reynolds number between micro- and macroscale flows. Yu et al. investigated the frictional pressure drop in circular fused silica microtubes of diameter 19.6 μm using nitrogen gas as the working fluid, and diameter 52.1 μm using both nitrogen gas and water [10]. Critical Reynolds numbers in the range $2000 < Re_{cr} < 6000$ were reported. Xu et al. explored laminar and transitional flow in microchannels of hydraulic diameters 30–344 μm, and concluded that characteristics agreed with conventional behavior in the range of parameters tested [11]. Transition to turbulence was observed to occur at $Re_{cr} \approx 2000$. Critically examining the detailed early gas-flow pressure drop measurements of Wu and Little [12] in trapezoidal microchannels of $D_h = 45.5$–83.1 μm, Obot concluded that transition occurs at a critical Reynolds number of 2290, consistent with macroscale convention [13]. The frictional pressure drop data of Liu and Garimella [14] in rectangular microchannels of hydraulic diameter 244–974 μm fabricated from Plexiglas suggest that transition occurs at a critical Reynolds number of 2000. Sharp and Adrian conducted an exhaustive study of transition to turbulence in circular fused silica microtubes of diameters between 50 and 247 μm [1]. Measurements included frictional pressure drop and mean/rms velocity fluctuation data collected using micro-PIV, using water, 1-propanol, and 20%-glycerol as working fluids. The data reveal conclusively that the critical Reynolds number lies in the range $Re_{cr} = 1800$–2300.

Several recent studies have explored the effect of viscous dissipation on laminar liquid flow in microchannels [15–17]. The influence of viscous heating on the liquid temperature and resulting effect on transport properties was investigated. Of particular note was the dependence of the liquid viscosity on temperature, with the observation that viscous heating can result in an apparent drop in the friction factor at the microscale. However, none of these studies investigated the transition from laminar to turbulent flow.

Much of the apparent discord concerning microscale effects on the critical Reynolds number, Re_{cr}, can be attributed to difficulties in minimizing experimental uncertainty. Certain sources of measurement error, though negligible at the macroscale, are amplified at small physical scales [1,18]. In the summary of prior work presented here, no study characterizing the onset of transition to turbulent flow has been reported for liquids in microchannels of nominal hydraulic diameter $D_h < 50$ μm. This study seeks to address the transition from laminar to turbulent flow in circular microchannels with nominal diameters ranging between 16 and 32 μm using water as the working fluid. Frictional pressure drop data were taken in the Reynolds number range $300 < Re < 3450$. The experimental apparatus and procedure were checked by verifying the laminar flow behavior $fRe = 64$ reported previously for laminar flows in microtubes [19]. The onset of transition was then identified by the deviation in the friction factor-Reynolds number product from this classical laminar result. A second, independent measure of the critical Reynolds number was also employed. This involved characterizing the fluid

mixed-mean temperature rise due to viscous heating over the microtube length. Since the viscous heating is dependent on the velocity profile, a deviation from the classical laminar flow profile can be deduced if the data are appropriately normalized. To the authors' knowledge, this is the first such determination of transition based on viscous heating-related thermal behavior in unheated microtubes.

2. Experimental setup and procedure

Experiments were undertaken to carefully characterize the frictional pressure drop for liquid flow in microtubes of nominal diameter less than 30 μm. The experimental apparatus consists of a high-pressure pump, PID controller, pressure transducer, valve, microtube of known length and inside diameter and liquid collection cylinder, as shown schematically in Fig. 1a. These components will now be described.

The fused silica circular microtubes were provided by Polymicro Technologies (Phoenix, AZ, USA). The microtubes are supplied with a manufacturer characterization of the inside and outside diameter at the two ends of the sample. As determined by the manufacturer, the diameter measurements never differed by more than 1 μm over the 1-m length. Since a previous investigation had revealed the possibility of substantial error in the vendor-supplied diameter data, diameters for all of the microtube samples used in this study were measured using scanning electron microscopy (SEM). Multiple diameter measurements were obtained from which an average was calculated. Against a calibration standard, these measurements are accurate to ±1 μm. Four tube diameters were explored as part of this study, whose vendor-supplied values were 14.5, 19.0, 25.5 and 30.0 μm. The corresponding SEM measurements of microtube diameters were 16.6, 19.7, 26.3 and 32.2 μm, respectively. Once scored and broken to the desired length (between 1.0 and 3.0 cm), the ends of the fused silica tube samples were carefully polished to remove burrs. Scanning electron micrographs of the two microtube diameter extremes ($D = 32.2$ and 16.6 μm) are shown in Fig. 2. The microtube wall thicknesses were much larger than the inside diameter for all samples, and a re-entrant flow condition existed.

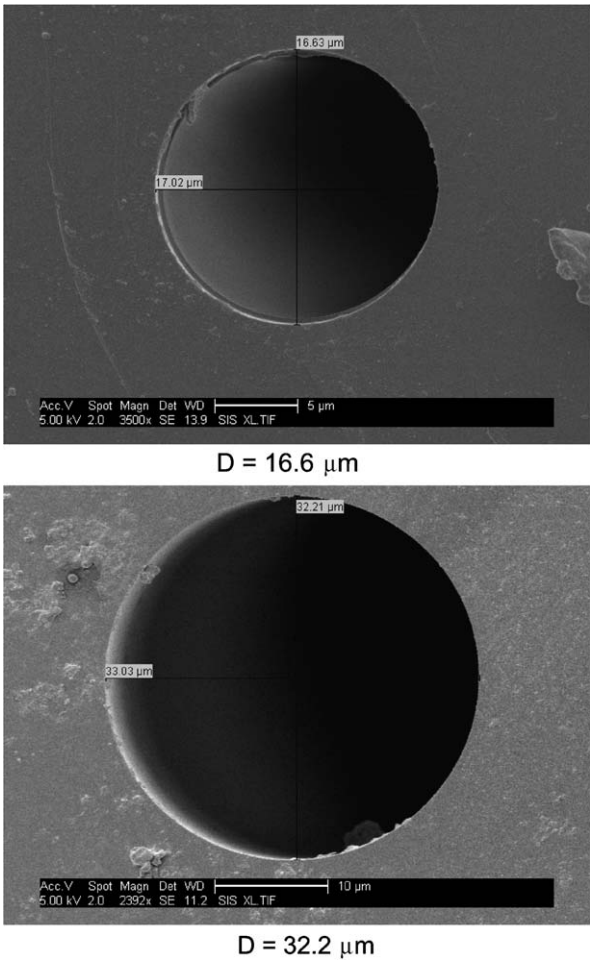

Fig. 2. Scanning electron micrographs of two microtube samples, $D = 16.6$ and 32.2 μm.

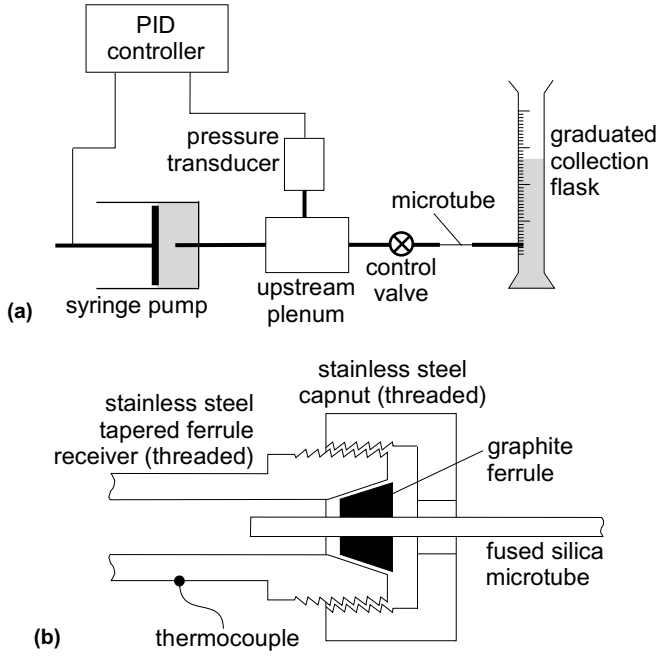

Fig. 1. Schematic of experimental apparatus.

Although no microtube wall roughness measurements were made as part of this study, previous investigations have reported such measurements for the same sample material and vendor used here. Brutin and Tadrist measured the surface roughness in Polymicro-supplied fused silica microtubes using atomic force microscopy (AFM) [18]. Measurements revealed the average roughness in a nominally 50 μm-diameter tube to be 10 nm. Cui and Silber-Li also report AFM measurements in polymicro fused silica tubes of nominal diameter 10 and 500 μm [20]. The average roughness of the two tube diameters was reported to be 70 and 7.1 nm, respectively, although difficulty was reported in adequately preparing the 10 μm-diameter tube

surface. Using the Brutin and Tadrist average roughness of 10 nm, the relative roughness for the tubes employed here ranges from 0.0003 to 0.0004 for the 16.6–32.2 μm diameter range explored. Thus, given the wall roughness data available, the tubes can probably be considered to be smooth-walled in the Reynolds number range investigated. Even if the less realistic average roughness of 70 nm reported by Cui and Silber-Li for the 10 μm tube is assumed, the largest relative roughness in this study (for the 16.6 μm-diameter tube) is 0.004, which may also be argued to be smooth-walled for the maximum flow Reynolds number of 3400 studied in this microtube.

The microtube samples were mounted between the reservoir of the high-pressure syringe pump and a graduated flask which served as spent fluid collection tube. The samples were held in place using graphite/vespel ferrules and stainless steel threaded connectors, as illustrated in Fig. 1b. The syringe pump was driven by a stepper motor using a reducer gear and a worm drive. The pump is capable of pressures up to 4100 atm (60 kpsi). A pressure transducer is connected to the reservoir on the upstream side of the microtube, and a PID (proportional–integral-derivative) controller receives input from the pressure transducer to maintain the syringe pump at a desired pressure setpoint. The controller maintains constant pressure to within the measurement accuracy of the pressure transducer, ±0.1% of full scale, or 410 kPa (60 psi).

All flow experiments were performed using distilled, deionized water. For each trial, the time required for a specified volume of fluid to flow through the microtube was measured using a stopwatch. Because of the small physical scale of the flow apparatus, direct measurements of the fluid temperature were not possible. The inlet and outlet mixed-mean temperatures were thus measured by K-type thermocouples firmly affixed to the stainless steel tubing, as shown in Fig. 1b. These temperatures were each recorded twice during the flow measurements, at the beginning and end of the measurement period. The arithmetic average of the inlet and outlet mean temperatures at both measurement times was used to determine the fluid viscosity μ and density ρ in the Reynolds number and friction factor calculations. Further, these temperature data were used in a novel thermal approach to independently determine the critical Reynolds number. This approach is outlined in a section to follow.

Using the measured/controlled values of total pressure drop across the microtube ΔP, measured volume flow ΔV over the elapsed time Δt, tube diameter D and tube length L, the Reynolds number Re and friction factor f were calculated from their definitions:

$$Re = \frac{4\rho\Delta V}{\pi\mu D\Delta t} \tag{1}$$

$$f = \frac{\pi^2 D^5 \Delta P \Delta t^2}{8\rho L \Delta V^2} - \frac{D}{L}\sum K_L \tag{2}$$

The term $\sum K_L$ in Eq. (2) represents the sum of minor loss coefficients corresponding to the re-entrant microtube inlet ($K_L = 0.8$) and exit ($K_L = 1.0$), and that associated with the hydrodynamic development length ($K_L = 1.3$) [21]. Thus, the sum of the minor loss coefficients is 3.1. These values are typical for macroscale flow, but they may carry more uncertainty than usual due to the assumption in applying them to microscale flow. In general, the minor losses contributed very little to the overall measured ΔP. However, for microtubes studies with the smallest L/D and at the highest laminar Reynolds number, the contribution from minor losses to the overall pressure drop amounted to 14%. Thus, the minor losses are not generally inconsequential, and were accounted for in all data.

Combining Eqs. (1) and (2), the product of the friction factor and Reynolds number may thus be expressed in terms of measured/controlled variables as

$$fRe = \frac{\pi D^4 \Delta P \Delta t}{2\mu L \Delta V} - \frac{4\rho\Delta V}{\pi\mu L\Delta t}\sum K_L \tag{3}$$

For classical laminar flow in a circular tube, the friction factor-Reynolds number product assumes a constant value of 64 [21]. The product fRe was plotted as a function of Reynolds number to determine both agreement with classical theory in the laminar regime, and the critical Reynolds number corresponding to transition from laminar to turbulent flow, Re_{cr}.

3. Experimental uncertainty

Characterization of the experimental uncertainty is particularly critical is reporting microscale measurements. A standard error analysis method was employed to determine the uncertainty in the results. As may be seen in Eq. (3), the dominant source of uncertainty is the microtube diameter, where the uncertainty in fRe is nominally a factor of four times the measurement error in D. Although the manufacturer reported the inner diameters of the microtubes accurate within 1–3 μm, the diameters were measured using a scanning electron microscope to within ±1 μm. As noted previously, the pressure drop across the microtube length ΔP was measured with an uncertainty of 410 kPa. This error is negligible for most of the data which required very high-pressures to generate the flow. At the minimum measured pressure drop, the transducer uncertainty yields a measurement error of 4.5%.

Fluid viscosity is nearly independent of pressure over the range of pressures explored [22]. However, the viscosity is temperature-dependent, and thus varies along the microtube length because of the viscous heating. Maximum mean fluid velocities in the microtube reached 130 m/s (for the smallest diameter, highest Reynolds number), causing significant rises in fluid temperature even over the short 1–3 cm tube lengths. As was done previously [19], the viscosity was evaluated at the average of the mixed-mean temperatures at the inlet and outlet of the microtube. However, since direct measurement of the fluid temperature was not possible, this evaluation is based on thermocouple mea-

surements made at the outer surface of the stainless steel tubing connecting the microtube at each end. The temperature rise thus measured reached a maximum for all measurements of 35 °C. Such a temperature rise results in a decrease in viscosity of nearly a factor of two.

The fluid density varies with both pressure and temperature. The maximum change in density with pressure amounted to 11% in the experiments reported here (for the smallest microtube diameter at the highest Reynolds number). Further, the drop in density due to viscous heating-induced fluid temperature rise was 2%. In the data reported, variations in density with both pressure and temperature were accounted for by evaluation of the density at the average fluid pressure and mixed-mean temperature, as with the viscosity. It should be noted that with regard to the experimental determination of fRe, fluid density only arises in the minor loss contribution to the overall pressure drop, as seen in Eq. (3). Therefore, for most conditions studied the fluid density variation is of no consequence.

Considering the contributing uncertainties in individual measurements outlined above, the composite experimental uncertainty for the fRe data reported here lies in the range 16–29%, with the highest uncertainty found in the experiments with the smallest microtube diameter (16.6 μm) at the highest Reynolds numbers. Note that these percentages are dominated by the ±1 μm uncertainty in the diameter, with all other variables contributing only modestly to the overall error.

4. Results and discussion

Flow measurements using eight different microtube samples were obtained. Table 1 illustrates the experimental test matrix. Approximately 240 data points were collected over the Reynolds number range 300–3400 for four different tube diameters. Tubes of different lengths were used for three of the four diameters. The minimum length-to-diameter ratio of all microtubes studied was $L/D \approx 600$.

Fig. 3 illustrates the experimentally measured friction factor-Reynolds number product as a function of Reynolds number for the four microtube diameters investigated. Data are plotted with error bars to illustrate the uncertainty in the measurements. As explained previously, the fractional uncertainty in fRe increases with decreasing tube diameter. The classical macroscale result of $fRe = 64$ for laminar flow in a circular tube is also shown.

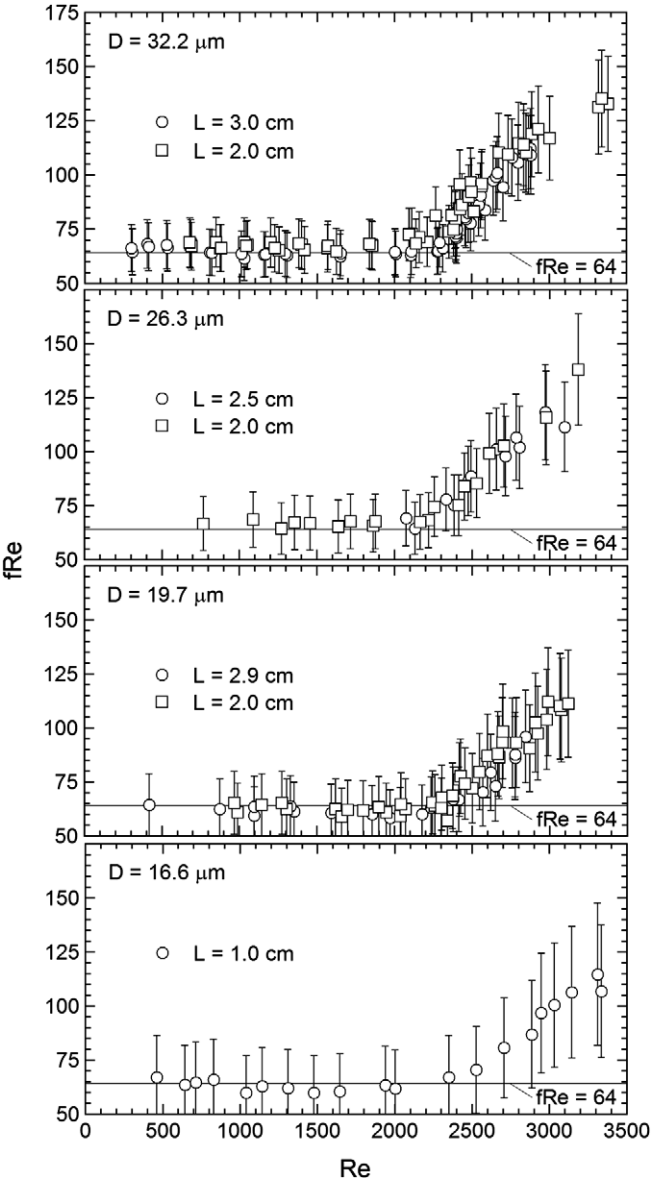

Fig. 3. Experimentally measured variation of the friction factor-Reynolds number product with Reynolds number.

Two distinct flow regimes are evident in the figure. At low Reynolds number, fRe is independent of Reynolds number and, well within the experimental uncertainty, equals the classical value of 64 for circular tubes. This laminar flow behavior is repeatable, and is found for all tube diameters. Further, there is little observable influence of the microtube length on the measured fRe, indicating the prevalence of a fully-developed flow over the majority of the microtube length for most tests. This is not surprising, since L/D for the microtube samples investigated ranged from 600 to 1470. At higher Reynolds numbers the friction factor-Reynolds number product deviates from that which is observed in the laminar flow regime, exhibiting a dependence on the flow Reynolds number. The critical Reynolds

Table 1
Matrix of experimental test conditions

Tube diameter (μm)	Tube length (cm)	Range of pressure drop (MPa)	Reynolds number range
16.6	1.0	27.6–213.6	400–3400
19.7	2.0	55.8–228.1	900–3100
19.7	2.9	41.3–241.9	400–2800
26.3	2.0	24.1–137.8	700–3200
26.3	2.5	68.9–137.8	2000–3100
32.2	2.0	13.8–102.0	600–3400
32.2	3.0	9.0–106.8	300–2900

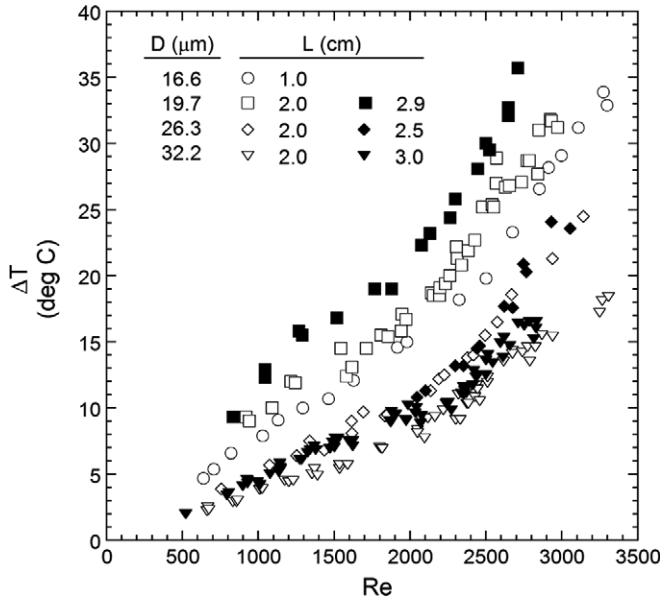

Fig. 4. Measured increase in the fluid mixed-mean temperature.

number that separates these two regimes ranges between $Re_{cr} = 2100$ and 2500 for all cases. Thus, from the data presented here, there is no evidence of either early or delayed transition to turbulence resulting from phenomena that may become significant at these physical scales. A slight dependence of Re_{cr} on microtube diameter may be observed in the data of Fig. 3; it appears that the critical Reynolds number may increase slightly with decreasing diameter. However, the variation is slight and is within the experimental error.

Fig. 4 presents the measured rise in fluid mixed-mean temperature, $\Delta T = T_{m,o} - T_{m,i}$, as a function of Reynolds number for the four microtube diameters studied. As stated previously, these measurements must be qualified somewhat, since the thermocouples were, by necessity, attached to the stainless steel tubing at the microtube inlet and exit as opposed to directly measuring the fluid temperature. As expected, the mean temperature rise ΔT increases monotonically with increasing Reynolds number. Further, the fluid temperature rise increases with increasing microtube length and decreasing microtube diameter. The viscous heating-induced temperature rise is significant, reaching 35 °C in some cases. Interestingly, the data as presented in Fig. 4 reveal no discernible variation in behavior between the laminar and turbulent flow regimes seen in the fRe data of Fig. 3.

If one assumes that the microtube wall is adiabatic, the viscous heating-induced rise in mixed-mean temperature over a known tube length L can be expressed as

$$\rho\bar{u}\pi R^2 c_p(T_{m,o} - T_{m,i}) = \int_0^L \int_0^R \mu\left(\frac{\partial u}{\partial r}\right)^2 2\pi r\,dr\,dx \qquad (4)$$

For a fully-developed laminar flow, the velocity profile is given as $u(r) = 2\bar{u}[1 - (r/R)^2]$, and the velocity gradient is thus $du/dr = -4\bar{u}r/R^2$. Substituting these expressions in Eq. (4), assuming constant thermophysical properties, and neglecting the hydrodynamic entrance region as being small relative to the total microtube length, yields, after rearrangement

$$Re/[Ec(L/D)] = 32 \qquad (5)$$

where Ec is the Eckert number based on the mean temperature rise, $\bar{u}^2/c_p(T_{m,o} - T_{m,i})$. It should be noted that despite the fact that the minimum L/D for these experiments was approximately 600, the hydrodynamic development length may not be insignificant for these relatively short channels. The maximum development length, L_{fd}, determined from $L_{fd}/D = 0.05Re$ [21] at $Re = 2300$ for the 16.6, 19.7, 26.3 and 32.2 μm diameter channels is 1.9, 2.3, 3.0 and 3.7 mm, respectively, constituting as much as 19% of the channel length. The liquid mean temperature rise data of Fig. 4 are recast in terms of the dimensionless viscous heating parameter $Re/[Ec(L/D)]$, and are plotted as a function of Re in Fig. 5. In this form the data show some interesting behavior. Again, two distinct flow regimes are evident. In the low-Re regime $Re/[Ec(L/D)]$ is approximately independent of Reynolds number with a magnitude somewhat less than 32 for all cases. This may be viewed as a confirmation of the laminar flow regime seen in the fRe data of Fig. 3. The experimentally observed magnitude of $Re/[Ec(L/D)]$ less than 32 in this laminar regime may be expected. The heat loss from the non-adiabatic walls results in a mixed mean temperature rise that is somewhat lower than what would be found for completely insulated walls. Further, the magnitude of $Re/[Ec(L/D)]$ is influenced by a finite entrance region, where the viscous heating-induced mean temperature rise is perhaps lower than in the fully-developed regime. (The steeper velocity gradients in the entrance region are confined to a small radial region in the microtube cross-section.)

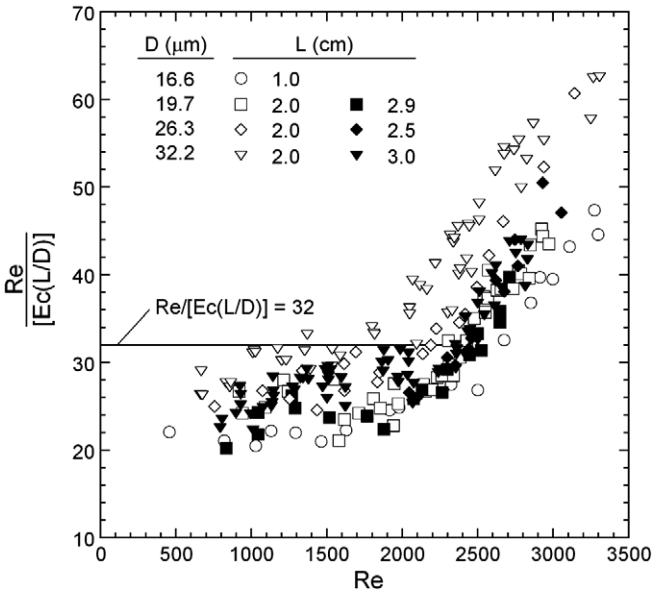

Fig. 5. Variation of the viscous heating parameter $Re/[Ec(L/D)]$ with Reynolds number.

The apparent dependence of $Re/[Ec(L/D)]$ on D and L in the laminar regime seen in Fig. 5 is thus not surprising, since the heat loss from the microtube and entrance effects are a function of microtube geometry (L and D), each tube resulting in a unique departure from the ideal case $Re/[Ec(L/D)] = 32$.

At high Reynolds numbers $Re/[Ec(L/D)]$ is observed in Fig. 5 to increase with Re, indicative of a fundamental change in the shape of the velocity profile and associated transport mechanism from that which prevails in laminar flow, with a corresponding increase in the viscous heating of the fluid. Again, this is suggestive of the onset of a turbulent flow regime, in keeping with the increase in fRe observed previously. This viscous heating-based indicator of transition from laminar to turbulent flow is fully independent of the frictional pressure drop data presented in Fig. 3. The transition between from laminar to turbulent flow regimes occurs in the range $Re_{cr} = 2100$–2500, consistent with the frictional pressure drop results. The data of Fig. 5 may also suggest a slight dependence of the critical Reynolds number on the microtube diameter. Transition occurs at somewhat higher Reynolds number as the microtube diameter decreases.

5. Conclusions

Measurements of the frictional pressure drop and viscous heating-induced temperature rise were made for water flowing through fused silica microtubes. Over 240 independent experimental conditions were explored for microtube diameters ranging from 16.6 to 32.2 μm spanning the Reynolds number range $300 < Re < 3400$. Classical laminar flow behavior was confirmed at low Reynolds numbers. The onset of transition from laminar to turbulent flow was observed using two independent approaches to occur at $Re_{cr} = 2100$–2500.

Acknowledgements

The authors would like to thank the Office of Research and Creative Activities (ORCA) at Brigham Young University for providing financial support of this project, and Richard Christiansen for collecting the SEM images.

References

[1] K.V. Sharp, R.J. Adrian, Transition from laminar to turbulent flow in liquid filled microtubes, Exp. Fluids 36 (2004) 741–747.
[2] X.F. Peng, G.P. Peterson, B.X. Wang, Frictional flow characteristics of water flowing through rectangular microchannels, Exp. Heat Transfer 7 (1994) 249–264.
[3] X.F. Peng, G.P. Peterson, B.X. Wang, Heat transfer characteristics of water flowing through rectangular microchannels, Exp. Heat Transfer 7 (1994) 265–383.
[4] T.M. Harms, M. Kazmierczak, F.M. Gerner, A. Hölke, H.T. Henderson, J. Pilchowski, K. Baker. Experimental Investigation of Heat Transfer and Pressure Drop through Deep Microchannels in a (1 1 0) Silicon Substrate, HTD-vol. 351, ASME, New York, 1997, pp. 347–357.
[5] S.-S. Hsieh, C.-Y. Lin, C.-F. Huang, H.-H. Tsai, Liquid flow in a micro-channel, J. Micromech. Microeng. 14 (2004) 436–445.
[6] G.M. Mala, D.Q. Li, Flow characteristics of water in microtubes, Int. J. Heat Fluid Flow 20 (1999) 142–148.
[7] R. Zeighami, D. Laser, P. Zhou, M. Asheghi, S. Devasenathipathy, T. Kenny, J. Santiago, K. Goodson, Experimental investigation of flow transition in microchannels using micron-resolution particle image velocimetry, Proc. 2000 Inter-Society Conference on Thermal Phenomena, vol. 2, IEEE, New York, 2000, pp. 148–153.
[8] H. Li, R. Ewoldt, M.G. Olsen, Turbulent and transitional velocity measurements in a rectangular microchannel using microscopic particle image velocimetry, Exp. Thermal Fluid Sci. 29 (2005) 435–446.
[9] D. Pfund, D. Rector, A. Shekarriz, A. Popescu, J. Welty, Pressure drop measurements in a microchannel, AIChE J. 46 (2000) 1496–1507.
[10] D. Yu, R. Warrington, R. Barron, T. Ameel, An experimental and theoretical investigation of fluid flow and heat transfer in microtubes, Proc. ASME/JSME Thermal Engineering Conf., vol. 1, ASME, New York, 1995, pp. 523–530.
[11] B. Xu, K.T. Ooi, N.T. Wong, W.K. Choi, Experimental investigation of flow friction for liquid flow in microchannels, Int. Commun. Heat Mass Transfer 27 (2000) 1165–1176.
[12] P. Wu, W.A. Little, Measurements of friction factor for the flow of gases in very fine channels used for micro miniature Joule–Thompson refrigerators, Cryogenics 23 (1983) 273–277.
[13] N. Obot, Toward a better understanding of friction and heat/mass transfer in microchannels – a literature review, Microscale Thermophys. Eng. 6 (2003) 155–173.
[14] D. Liu, S. Garimella, Investigation of liquid flow in microchannels, AIAA Paper 2002-2776, AIAA, New York, 2002.
[15] B. Xu, K.T. Ooi, C. Mavriplis, M.E. Zaghloul, Evaluation of viscous dissipation in liquid flow in microchannels, J. Micromech. Microeng. 13 (2003) 53–57.
[16] J. Koo, C. Kleinstreuer, Viscous dissipation effects in microtubes and microchannels, Int. J. Heat Mass Transfer 47 (2004) 3159–3169.
[17] G.L. Morini, Viscous heating in liquid flows in microchannels, Int. J. Heat Mass Transfer 48 (2005) 3637–3647.
[18] D. Brutin, L. Tadrist, Experimental friction factor of a liquid flow in microtubes, Phys. Fluids 15 (2003) 653–661.
[19] J. Judy, D. Maynes, B.W. Webb, Characterization of frictional pressure drop for liquid flow through microchannels, Int. J. Heat Mass Transfer 45 (2002) 3477–3489.
[20] H.-H Cui, Z.-H. Silber-Li, Flow characteristics of liquids in microtubes driven by a high pressure, Phys. Fluids 16 (2004) 1803–1810.
[21] R.D. Blevins, Applied Fluid Dynamics Handbook, Van Nostrand Reinhold, New York, 1984.
[22] P.W. Bridgman, The effect of pressure on the viscosity of forty-three pure liquids, Proc. Amer. Acad. 61 (1926) 57–99.